IEEE Access
Multidisciplinary | Rapid Review | Open Access Journal

Received August 3, 2020, accepted August 5, 2020, date of publication October 5, 2020, date of current version October 14, 2020.

Digital Object Identifier 10.1109/ACCESS.2020.3028559

Capacitance Tuning Method for Maximum Output Power in Multiple-Transmitter Wireless Power Transfer System

SEON-JAE JEON AND DONG-WOOK SEO
Department of Radio Communication Engineering, Korea Maritime and Ocean University, Busan 49112, South Korea

Corresponding author: Dong-Wook Seo (dwseo@kmou.ac.kr)

This work was supported by the National Research Foundation of Korea (NRF) grant funded by the Korea government (MSIT) (No. 2018R1C1B6003854).

ABSTRACT It is common knowledge that wireless power transfer (WPT) systems with multiple transmitters (Txs) and a single receiver (Rx) have robust efficiency against lateral misalignment. However, the unnecessary coupling among Txs in actual multi-Tx WPT systems causes transmission efficiency degradation, and then additional tuning work is required to adjust some system parameters, such as the phase or frequency of Tx sources. Moreover, the frequency-splitting phenomenon caused by over-coupling between the Txs and Rx still occurs in multi-Tx systems. Thus, output power degradation is inevitable in the over-coupled state. In this article, we propose an optimal capacitance tuning method that is applicable to multi-Tx WPT systems. A multi-Tx WPT system tuned with the optimal capacitances, which are obtained from the critical coupling condition between Txs and Rx, not only compensates the inner coupling among Txs but also achieves the maximum output power in the over-coupled state. To verify the validity of the proposed method, we implemented two-and three-Tx and single Rx WPT systems and measured the output power of load with respect to the Rx position along the x- and y-axes. As a result, with the proposed method without any changes in the operating frequency or phase, the systems could deliver higher output power than the conventional phase-controlled system. In particular, with the proposed method, the systems maintained the constant maximum transmission efficiency of 80% in the over-coupled state.

INDEX TERMS Magnetic beamforming, multiple transmitter, maximum output power, optimal tuning, power transfer efficiency, transmission efficiency, wireless power transfer.

I. INTRODUCTION

Wireless power transfer (WPT) systems have great advantages, offering the convenience of mobility and lightness for many devices without electronic cables in daily life. Nowadays, WPT technology is widely used in vehicles, medical devices, and portable electronic devices [1]–[5]. Nevertheless, there is still a fundamental problem that typical WPT systems with a single transmitter (Tx) and receiver (Rx) have a maximum output power only at a specific distance corresponding to critical coupling between Tx and Rx [6]. In particular, lateral misalignment between Tx and Rx causes the mutual coupling to be significantly weaker, resulting in reduced output power [7]–[11].

To overcome the misalignment issue, various studies on coil structure have been conducted [12]–[15]. In [12], Budhia *et al.* proposed the double-D coil (DD coil) for a bipolar coupled arrangement. DD coils maintain a high magnetic flux with a wider area than conventional circular coils. Similarly, square DD coils were also implemented with a circular form to increase the tolerance to lateral misalignment [13]. The work reported in [14] explained the interrelation between the coupling factor and geometry of ferrite and aluminum. In [15], Kim *et al.* designed an asymmetric coil structure with the variation of width and an additional inner coil to achieve a higher quality factor than that of a conventional uniform one. However, it is difficult to implement the exact structures proposed in these studies according to variation of coil size because of complicated structures. On the other hand, multiple-transceiver configurations using two or more Txs or Rxs have also been studied to overcome the misalignment issue. In [16] and [17], it was experimentally verified that a multi-Tx system using two or more Txs transfers power more efficiently with a wider area than a single-Tx system. It is well-known that, for high efficiency in a multi-Tx system, the amplitude of the input signal should be adjusted in

The associate editor coordinating the review of this manuscript and approving it for publication was Francisco Perez-Pinal.

proportion to the coupling coefficient between the Txs and Rx [18]. Similarly, in [19], it was verified that the current ratio of transmitters should be equal to the coupling coefficient ratio for the maximum efficiency. However, because the inner coupling coefficient among Txs is not zero in actual situations, the additional reactance in Txs causes signal delay and output power reduction. Thus, an actual multi-Tx system requires not only amplitude but also phase adjustment for each Tx [18]. Because this method adjusts the magnitude and phase of each source, similar to the beamforming technique of array antennas, it is often called magnetic beamforming [18]. In [20] and [21] the adaptive phase control method according to the Rx position in a multi-Tx system was studied. However, because the unnecessary reactance generated by inner coupling among Txs still remains, the phase-controlled system cannot achieve the ideal maximum output power.

To eliminate the effect of inner coupling among Txs, non-inner coupling arrangements have been studied [22]–[25]. In [22], the bipolar pad (BPP) scheme that is a decoupling structure with partially overlapping coils based on the DD coil was proposed. This structure creates magnetic decoupling between overlapped coils by the opposite flux of each outside coil. Furthermore, in [23], the maximum efficiency point tracking (MEPT) system with BPP coils which is useful to electronic vehicles was derived. In [24] and [25], a quadrupole loop coil was introduced, which implements the decoupling by the opposite direction of each current. However, these arrangements require an exact symmetry structure. In addition, Ahn and Hong proposed the frequency tuning method to track the shifted resonance frequency by inner coupling among Txs and Rxs [26]. However, the frequency tuning method may violate the allowable narrow bandwidth in high-frequency (HF) band such as 6.78 MHz or 13.56 MHz. Similarly, the resonant capacitance tuning methods had also been introduced [27], [28]. In [27], the authors theoretically and experimentally demonstrated the compensation method for inner coupling among Rxs. In [28], the precise optimization system was implemented with the iteration algorithm. These methods are implementable regardless of coil size, structure, and narrow frequency band.

On the other hand, there is the common problem for the WPT systems that the output power is reduced by frequency-splitting phenomenon in the over-coupled state, which has stronger coupling than critical coupling between the Tx and Rx [6], [29], [30]. This problem still occurs in multi-coil WPT systems [31]. It means that multi-Tx systems can also deliver the maximum output power only in certain area satisfying critical coupling. Recently, the optimal loads for multi-Tx systems to improve the output power and efficiency in the over-coupled state have been studied [32], [33]. In [32], the optimal load that is applicable to multi-Tx system was derived. This work also verified the method to determine the optimal load for two-, three-, and four-Tx systems in the over-coupled state. However, the effect of inner coupling among Txs was not considered in this study. In [33], the MEPT for multi-Tx WPT systems was introduced. The optimal load value based on system energy efficiency was implemented with the duty cycle topology of a DC-DC converter at 100 kHz. However, although the optimal current source, which has no impact on the signal delay caused by inner coupling, was implemented with an inductor-capacitor-capacitor (LCC) inverter, the unnecessary reactance caused by the inner coupling among Txs still remained in each Tx.

In this article, we propose an optimal capacitance tuning method for multi-Tx systems. A multi-Tx system tuned with the optimal capacitance, which is derived from the critical coupling condition based on the maximum transmission efficiency, not only completely compensates the unnecessary reactance caused by coupling among Txs but also has strong tolerance to frequency-splitting phenomenon in the over-coupled state. Thus, it can achieve the maximum output power in a wide area including the over-coupled state. In addition, it is useful for the narrow HF band.

In Section II, we concretely derive the expression of the optimal capacitance in a two-Tx system and then expand the expression for n-Tx system. In Section III, we analyze the issues of the conventional two-Tx system and strengths of the proposed system tuned with the optimal capacitance by using MATLAB and then verify the validity of the proposed system through measured and simulated results for the transmission coefficient and efficiency in two- and three-Tx systems. Finally, some conclusions are drawn in Section IV.

II. THEORETICAL ANALYSIS OF PROPOSED METHOD

In this section, we derive the optimal capacitance for a multi-Tx WPT system. First, we obtain the critical coupling coefficient through the transmission efficiency in a two-Tx system and then derive the free resonant angular frequencies that satisfy the critical condition. Next, the generalized formula for n-Tx system is derived.

A. ANALYSIS OF TWO-TX SYSTEM

Among the various compensation topologies in resonant inductive power transfer (RIPT) technology, the series-series (SS) compensation topology can perform the maximum output power with less complexity of system control and component count than other topologies [34]–[36]. Hence, in this study, the multi-Tx systems were implemented with SS topology. Figure 1 shows the general multi-Tx WPT system using two Txs. The two Tx-coils (L_{T1} and L_{T2}) and one Rx coil (L_R) are magnetically coupled by M_{12}, M_{1R}, and M_{2R}. Each coil has parasitic resistance (R_{T1}, R_{T2}, and R_R) and resonates at the operating frequency by using the resonant capacitances (C_{T1}, C_{T2}, and C_R). The Txs and Rx are connected with the voltage source (V_1 and V_2), source resistance (R_S), and load (R_L) in series.

The matrix equation through Kirchhoff's voltage law (KVL) for the two-Tx system is given by

$$\begin{bmatrix} V_1 \\ V_2 \\ 0 \end{bmatrix} = \begin{bmatrix} Z_{Tx,1} & j\omega M_{12} & -j\omega M_{1R} \\ j\omega M_{12} & Z_{Tx,2} & -j\omega M_{2R} \\ -j\omega M_{1R} & -j\omega M_{2R} & Z_{Rx} \end{bmatrix} \begin{bmatrix} I_{T1} \\ I_{T2} \\ I_R \end{bmatrix}, \quad (1)$$

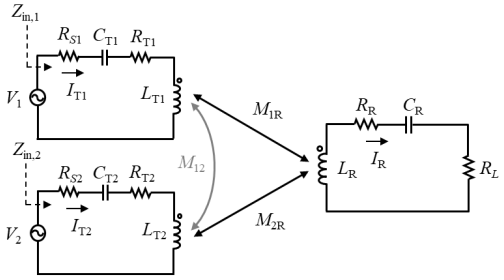

FIGURE 1. Equivalent circuit of two-Tx WPT system.

where $Z_{Tx,1} = R_{S1} + R_{T1} + j\omega L_{T1} + 1/j\omega C_{T1}$, $Z_{Tx,2} = R_{S2} + R_{T2} + j\omega L_{T2} + 1/j\omega C_{T2}$, and $Z_{Rx} = R_R + R_L + j\omega L_R + 1/j\omega C_R$ are the total impedances of the primary, secondary Txs and Rx, respectively.

It is well-know that I_{T1} and I_{T2} (or V_1 and V_2) must be adjusted in accordance with the ratio between M_{1R} and M_{2R} to achieve the maximum efficiency [18], [19] as follows:

$$\frac{I_{T2}}{I_{T1}} = \frac{M_{2R}}{M_{1R}} = \alpha. \tag{2}$$

If the amplitude of the voltage sources are adjusted to satisfy the optimum current ratio of (2), I_{T2} and M_{2R} can be represented with αI_{T1} and αM_{1R}, respectively. On the other hand, despite the condition of (2), $j\omega M_{12}$ terms caused by inner coupling between L_{T1} and L_{T2} in (1) still remain, and they lead to deviation of the resonance frequency from the operating frequency. Consequently, $j\omega M_{12}$ terms degrade the output power. Therefore, the terms in each Tx should be eliminated for the maximum output power.

The input impedances $Z_{in,1}$ and $Z_{in,2}$ are given by

$$Z_{in,1} = V_1/I_{T1} = R_{Tx,1} + j\omega L_{Tx,1} + \frac{1}{j\omega C_{T1}} - j\omega M_{1R}\frac{I_R}{I_{T1}}, \tag{3a}$$

$$Z_{in,2} = V_2/I_{T2} = R_{Tx,2} + j\omega L_{Tx,2} + \frac{1}{j\omega C_{T2}} - j\omega M_{1R}\frac{I_R}{I_{T1}}, \tag{3b}$$

where $L_{Tx,1} = L_{T1} + M_{12}.\alpha$, $L_{Tx,2} = L_{T2} + M_{12}/\alpha$, $R_{Tx,1} = R_{S1} + R_{T1}$, and $R_{Tx,2} = R_{S2} + R_{T2}$. If C_{T1} and C_{T2} are replaced with $C_{Tx,1} = 1/(\omega_0^2 L_{Tx,1})$ and $C_{Tx,2} = 1/(\omega_0^2 L_{Tx,2})$, then the effect of M_{12} can be eliminated.

For simple circuit analysis, assume that all the Txs are identical ($L_{T1} = L_{T2} = L_T$ and $R_{Tx,1} = R_{Tx,2} = R_{Tx} = R_T + R_S$). Equation (1) can be rewritten as

$$\begin{bmatrix} V_1 \\ V_2 \\ 0 \end{bmatrix} = \begin{bmatrix} R_{Tx} & 0 & -j\omega_0 M_{1R} \\ 0 & R_{Tx} & -j\omega_0 M_{1R}\alpha \\ -j\omega_0 M_{1R} & -j\omega_0 M_{1R}\alpha & R_{Rx} \end{bmatrix} \times \begin{bmatrix} I_{T1} \\ \alpha I_{T1} \\ I_R \end{bmatrix}, \tag{4}$$

where $R_{Rx} = R_R + R_L$. From (4), the Rx current I_R is obtained by

$$I_R = \frac{j\omega_0 M_{1R} I_{T1}\left(1+\alpha^2\right)}{R_{Rx}}. \tag{5}$$

Therefore, the output power is expressed as

$$P_L = \frac{1}{2}|I_R|^2 R_L = \frac{\omega_0^2 M_{1R}^2 I_{T1}^2 (1+\alpha^2)^2 R_L}{2R_{Rx}^2}. \tag{6}$$

From (4), the input power is also obtained by

$$P_{in} = \frac{1}{8}\cdot\frac{|V_1|^2 + |V_2|^2}{R_S} = \frac{\left(1+\alpha^2\right)\cdot\left\{R_{Tx} + \frac{\omega_0^2 M_{1R}^2(1+\alpha^2)}{R_{Rx}}\right\}^2}{8R_S}\cdot I_{T1}^2. \tag{7}$$

For the two-Tx WPT system with the optimum current ratio and non-inner coupling, the transmission effciency, a ratio of P_{out} to P_{in}, is expressed as

$$\eta = \frac{4R_S R_L\,\omega_0^2 M_{1R}^2\left(1+\alpha^2\right)}{\left\{R_{Tx}R_{Rx} + \omega_0^2 M_{1R}^2\left(1+\alpha^2\right)\right\}^2}. \tag{8}$$

By differentiating (8) with repect to k_{1R}, which is $M_{1R}/\sqrt{L_T L_R}$, the critical coupling coefficient between the primary Tx coil and Rx coil is obtained as

$$k_{1R,cri} = \frac{1}{\sqrt{Q_T Q_R\left(1+\alpha^2\right)}}, \tag{9}$$

where $Q_T = \omega_0 L_T/R_{Tx}$ and $Q_R = \omega_0 L_R/R_{Rx}$ are the loaded quality factors of the Tx and Rx, respectively. The critical coupling coefficient of the ideal two-Tx WPT system is lower than that of a single-Tx system, which is (9) in [36]. That is, due to the addition of the $(1 + \alpha^2)$ term, a multi-Tx WPT system can be more efficient for a wider area than a single-Tx system.

By substituting (9) into (8), we get the maximum transmission efficiency as

$$\eta_{max} = \frac{R_S R_L}{(R_T + R_S)(R_R + R_L)}. \tag{10}$$

As shown in (10), the ideal achievable maximum transmission efficiency of the two-Tx system increases as the parasitic resistances R_T and R_R are smaller than the source and load resistances R_S and R_L as in the conventional single-Tx WPT system.

However, despite the extremely small parasitic resistances, the maximum efficiency of (10) can be achieved only under the critical coupling condition of (9). In the over-coupled state, the frequency-splitting phenomenon still occurs and results in efficiency degradation. That is, even the optimum current ratio of (2) and non-inner coupling condition do not guarantee the maximum output power in the over-coupled state.

In a previous work [37], a resonant capacitance tuning method was introduced that allows only a single-Tx system to achieve the maximum output power in the over-coupled state. In this work, we derive an optimum capacitance that is usable for multi-Tx systems regardless of the number of Txs.

First, the modulus ratio of I_R to I_{T1} at the operating frequency in the two-Tx WPT system of Fig. 1 is given by

$$\left|\frac{I_R}{I_{T1}}\right|_{\omega=\omega_0} = \left|\frac{j\omega_0 M_{1R}\left(1+\alpha^2\right)}{j\omega_0 L_R + \frac{1}{j\omega_0 C_R} + R_{Rx}}\right|. \tag{11}$$

Next, substituting (9) into (11) leads to the critical current condition between the primary Tx and Rx,

$$\left|\frac{I_R}{I_{T1}}\right|_{\substack{\omega=\omega_0 \\ k_{1R}=k_{1R,cri}}} = \sqrt{\frac{R_{Tx}}{R_{Rx}}\left(1+\alpha^2\right)}. \tag{12}$$

Letting (11) equal (12) and using the definition of the free resonant angular frequency of the Rx, $\omega_R = 1/\sqrt{L_R C_R}$, gives

$$\sqrt{\frac{R_{Tx}}{R_{Rx}}\left(1+\alpha^2\right)} = \left|\frac{j\omega_0 M_{1R}\left(1+\alpha^2\right)}{j\omega_0 L_R + \frac{\omega_R^2 L_R}{j\omega_0} + R_{Rx}}\right|. \tag{13}$$

Finally, solving for ω_R gives

$$\omega_R = \omega_0\sqrt{1 \pm \sqrt{k_{1R}^2 Q_T Q_R^{-1}\left(1+\alpha^2\right) - Q_R^{-2}}}. \tag{14}$$

On the other hand, to derive the free resonant angular frequency of the primary Tx, ω_{T1}, the ratio of V_1 to I_R at the operating frequency is given by

$$\left|\frac{V_1}{I_R}\right|_{\omega=\omega_0} = \left|\left(j\omega_0 L_{Tx,1} + \frac{1}{j\omega_0 C_{Tx,1}} + R_{Tx}\right)\frac{I_{T1}}{I_R} - j\omega_0 M_{1R}\right|. \tag{15}$$

Replacing $C_{Tx,1}$ with $1/(\omega_{T1}^2 L_{Tx,1})$ and substituting (12) into (15) gives

$$\left|\frac{V_1}{I_R}\right|_{\omega=\omega_0} = \left|\left(j\omega_0 L_{Tx,1} + \frac{j\omega_{T1}^2 L_{Tx,1}}{\omega_0} + R_{Tx}\right) \times \sqrt{\frac{R_{Tx}}{R_{Rx}}\left(1+\alpha^2\right)} - j\omega_0 M_{1R}\right|. \tag{16}$$

By inserting (9) into (15), the ratio at the critical coupling gives

$$\left|\frac{V_1}{I_R}\right|_{\substack{\omega=\omega_0 \\ k_{1R}=k_{1R,cri}}} = 2\sqrt{\frac{R_{Tx}R_{Rx}}{1+\alpha^2}}. \tag{17}$$

Comparing (16) and (17) yields

$$\omega_{T1} = \omega_0\sqrt{1 \pm \sqrt{Q_{Tx,1}^{-2}\left\{k_{1R}^2 Q_T Q_R\left(1+\alpha^2\right) - 1\right\}}}, \tag{18}$$

where $Q_{Tx,1} = \omega_0 L_{Tx,1}/R_{Tx}$. Similarly, we can get the free resonant angular frequency of the secondary Tx ω_{T2} as follows:

$$\omega_{T2} = \omega_0\sqrt{1 \pm \sqrt{Q_{Tx,2}^{-2}\left\{k_{1R}^2 Q_T Q_R\left(1+\alpha^2\right) - 1\right\}}}, \tag{19}$$

where $Q_{Tx,2} = \omega_0 L_{Tx,2}/R_{Tx}$.

B. ANALYSIS OF N-Tx SYSTEM

Figure 2 shows the configuration of the n-Tx WPT system. If the multi-Tx WPT system has the optimum current ratio of (2), and M_{1R} is the reference mutual inductance, the i^{th} mutual inductance M_{iR} and current I_{Ti} are equal to $\alpha_i M_{1R}$ and $\alpha_i I_{T1}$, respectively.

Writing Kirchhoff's equation for the $n+1$ loops in Fig. 2 gives the following matrix equation:

$$\begin{bmatrix} V_1 \\ V_2 \\ \vdots \\ V_n \\ 0 \end{bmatrix} = \begin{bmatrix} Z_{Tx,1} & j\omega M_{12} & \cdots & j\omega M_{1n} & -j\omega M_{1R} \\ j\omega M_{21} & Z_{Tx,2} & \cdots & j\omega M_{2n} & -j\omega M_{1R}a_2 \\ \vdots & \vdots & \ddots & \vdots & \vdots \\ j\omega M_{n1} & j\omega M_{n2} & \cdots & Z_{Tx,n} & -j\omega M_{1R}a_n \\ j\omega M_{1R} & j\omega M_{1R}a_2 & \cdots & j\omega M_{1R}a_n & Z_{Rx} \end{bmatrix} \times \begin{bmatrix} I_{T1} \\ a_2 I_{T1} \\ \vdots \\ a_n I_{T1} \\ I_R \end{bmatrix}. \tag{20}$$

Under the assumption that all the Txs are identical, the i^{th} input impedance $Z_{in,i}$ is expressed by using the i^{th} row of (20) as

$$Z_{in,i} = V_i/I_{Ti} = R_{Tx} + j\omega L_{Tx,i} + \frac{1}{j\omega C_{Ti}} - j\omega M_{1R}\frac{I_R}{I_{T1}}, \tag{21}$$

where

$$L_{Tx,i} = L_T + \frac{1}{\alpha_i}\sum_{k=1,k\neq i}^{n}\alpha_k M_{ik}. \tag{22}$$

If C_{Ti} is replaced with $1/(\omega_0^2 L_{Tx,i})$, (20) can be rewritten as

$$\begin{bmatrix} V_1 \\ V_2 \\ \vdots \\ V_n \\ 0 \end{bmatrix} = \begin{bmatrix} R_{Tx} & 0 & \cdots & 0 & -j\omega_0 M_{1R} \\ 0 & R_{Tx} & \cdots & 0 & -j\omega_0 M_{1R}\alpha_2 \\ \vdots & \vdots & \ddots & \vdots & \vdots \\ 0 & 0 & \cdots & R_{Tx} & -j\omega_0 M_{1R}\alpha_n \\ j\omega_0 M_{1R} & j\omega_0 M_{1R}\alpha_2 & \cdots & j\omega_0 M_{1R}\alpha_n & R_{Rx} \end{bmatrix} \times \begin{bmatrix} I_{T1} \\ \alpha_2 I_{T1} \\ \vdots \\ \alpha_n I_{T1} \\ I_R \end{bmatrix}. \tag{23}$$

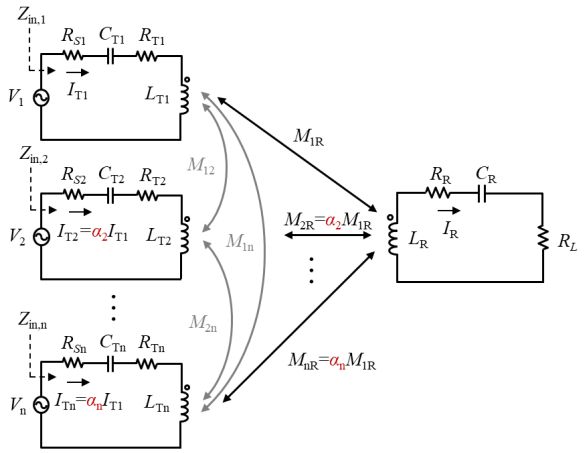

FIGURE 2. Equivalent circuit of *n*-Tx WPT system.

By using (23), the transmission efficiency is derived as

$$\eta = \frac{4\,|I_{\mathrm{R}}|^2 R_S R_L}{\sum_{k=1}^{n} |V_{\mathrm{k}}|^2} = \frac{4R_S R_L\,\omega_0^2 M_{1\mathrm{R}}^2 \left(1+\sum_{k=2}^{n}\alpha_k^2\right)}{\left\{R_{\mathrm{Tx}}R_{\mathrm{Rx}} + \omega_0^2 M_{1\mathrm{R}}^2\left(1+\sum_{k=2}^{n}\alpha_k^2\right)\right\}^2}. \tag{24}$$

By differentiating (24) with repect to $k_{1\mathrm{R}}$, the critical coupling coefficient is obtained as

$$k_{1\mathrm{R,cri}} = \frac{1}{\sqrt{Q_{\mathrm{T}}Q_{\mathrm{R}}\left(1+\sum_{k=2}^{n}a_k^2\right)}}. \tag{25}$$

Similar to the two-Tx system, the free resonant angular frequencies of the resonators are derived from the critical conditions for $|I_{\mathrm{R}}/I_{\mathrm{Ti}}|$ and $|V_{\mathrm{i}}/I_{\mathrm{R}}|$ as follows

$$\omega_{\mathrm{Ti}} = \omega_0\sqrt{1 \pm \sqrt{Q_{\mathrm{Tx,i}}^{-2}\left\{k_{1\mathrm{R}}^2 Q_{\mathrm{T}}Q_{\mathrm{R}}\left(1+\sum_{k=2}^{n}a_k^2\right)-1\right\}}}, \tag{26}$$

$$\omega_{\mathrm{R}} = \omega_0\sqrt{1 \pm \sqrt{k_{1\mathrm{R}}^2 Q_{\mathrm{T}}Q_{\mathrm{R}}^{-1}\left(1+\sum_{k=2}^{n}a_k^2\right)-Q_{\mathrm{R}}^{-2}}}. \tag{27}$$

Finally, the optimal capacitances for the i^{th} Tx and Rx are obtained as

$$C_{\mathrm{Tx,i,opt}} = \frac{1}{\omega_{\mathrm{Ti}}^2 L_{\mathrm{Tx,i}}}, \tag{28}$$

$$C_{\mathrm{R,opt}} = \frac{1}{\omega_{\mathrm{R}}^2 L_{\mathrm{R}}}. \tag{29}$$

III. EXPERIMENTAL SETUP AND RESULTS

In this section, we analyze the strengths of the proposed optimal capacitance by comparing it with the conventional resonant capacitance in the two-Tx WPT system and then verify its validity through simulated and measured results.

TABLE 1. Parameters for simulation and measurement.

Symbol	Notes	Values
f_0	operating frequency	6.78 MHz
R_S R_L	source and load resistance	1 Ω
L_{T} L_{R}	Tx and Rx coil inductances	1.11 μH
R_{T} R_{R}	Tx and Rx coil ESRs	0.15 Ω

A. ANALYSIS OF TWO-Tx SYSTEM

Consider the two-Tx system shown in Fig. 1, which has the parameters in Table I satisfying the optimum current ratio of (2). The coil inductance of 1.11 μH that is suitable for the low power applications such as the wearable and portable devices [38], [39] was chosen in this study. The transmission efficiency of the two-Tx system with respect to the coupling coefficient between each Tx and Rx, $k_{1\mathrm{R}}$ and $k_{2\mathrm{R}}$, was calculated by using MATLAB. Figures 3(a) and 3(b) show the transmission efficiency of the two-Tx system with an inner coupling coefficient of 0.03 and non-inner coupling, respectively. As expected, the system with inner coupling shows efficiency of only about 60%, whereas that without inner coupling reaches 80% in the area near the critical coupling coefficient. That is, the inner coupling degrades the output power even though the optimum current ratio condition is applied in the multi-Tx system. Thus, the inner coupling among Txs must be eliminated to achieve the maximum transmission efficiency. However, despite the non-inner coupling, efficiency degradation still occurs in the areas with $k_{1\mathrm{R}}$ (or $k_{2\mathrm{R}}$) > 0.04, because of the frequency splitting phenomenon in the over-coupled state. This means that although the multi-Tx system satisfies non-inner coupling among Txs, it achieves the maximum output power only in a certain area. By constrast, the proposed system tuned with the optimal capacitance maintains 80% of the maximum efficiency in areas with $k_{1\mathrm{R}}$ (or $k_{2\mathrm{R}}$) > 0.02 and $k_{1\mathrm{R}}$ & $k_{2\mathrm{R}} > 0.02$ as shown in Fig. 3(c). Therefore, these findings demonstrate that the proposed optimal capacitance not only eliminates the inner coupling between Txs but also enables the multi-Tx system to achieve the maximum output power in the over-coupled state.

Figure 4 shows the experimental setup for transmission coeffcient S_{21} to validate the strong tolerance to the frequency-splitting phenomenon in the proposed system tuned with the optimal capacitance. All of the coils used in the experiment were printed on an FR-4 substrate and had the parameter values shown in Table I. The coil dimensions, line width, and gap between lines were 95.7 mm × 105.7 mm, 5.7 mm, and 2.4 mm, respectively. The network analyzer and chip capacitors used in the experiment are additionally summarized in Table II. L-section matching networks were used to transform the desired source (or load) resistance to the impedance of the SMA connector, 50 ohms, as shown in Fig. 5 [40].

Figure 6 shows the three cases in accordance with the Rx position. In Case#1, the Rx was perfectly aligned with Tx1 as

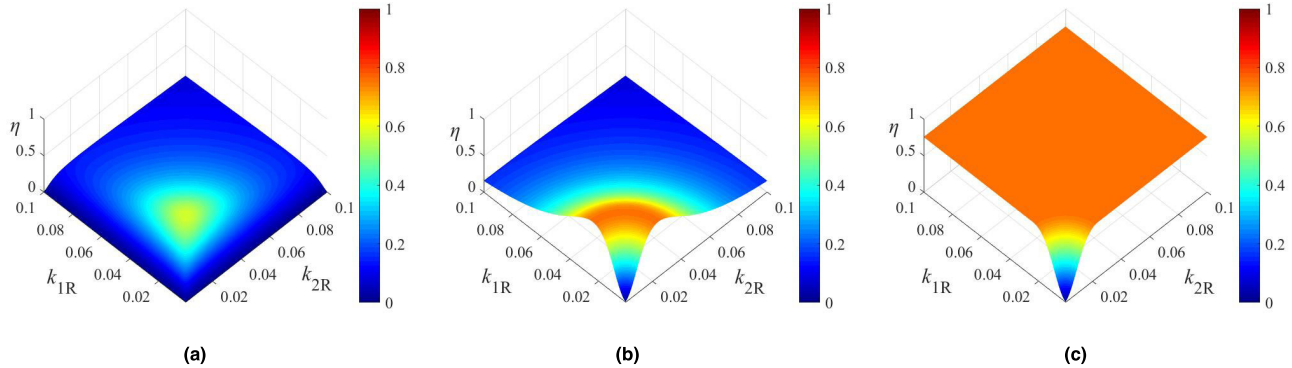

FIGURE 3. Calculated transmission efficiency with respect to variation of k_{1R} and k_{2R} in two-Tx system: the conventional system using 6.78 MHz resonant capacitance in cases of (a) $k_{12} = 0.03$ and (b) $k_{12} = 0$, the proposed system tuned with the optimal capacitance in case of (c) $k_{12} = 0.03$.

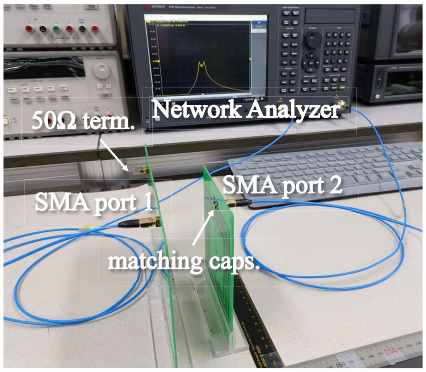

FIGURE 4. Measurement setup for transmission coefficient in two-Tx system.

TABLE 2. Details of simulation and measurement.

Instrument or Parts	Model or Type	Note
Network analyzer	Keysight E5071C	9 kHz–4.5 GHz
Calibration kit	Keysight 85052C	DC-26.5 GHz
Coaxial cable	RG 405	DC-18 GHz
Coils	FR-4 substrate	Dim.: 95.7 mm × 105.7 mm
Capacitors	Murata GRM series	Dim.: 1.6 mm × 0.8 mm

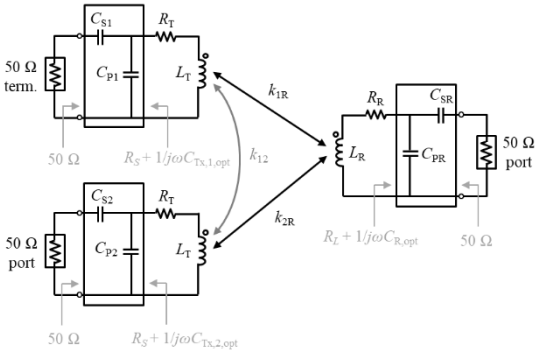

FIGURE 5. L-section matching networks to connect with 50Ω SMA ports in two-Tx WPT system.

shown in Fig. 6 (a). Thus, k_{1R} was significantly larger than k_{2R}. In Case#2, shown in Fig. 6 (b), the Rx was moved slightly along the y-axis, so it was not aligned with Tx1. In this case, k_{1R} was smaller than in the case of perfect alignment between Tx1 and the Rx. In Case#3, the Rx was located at the center of

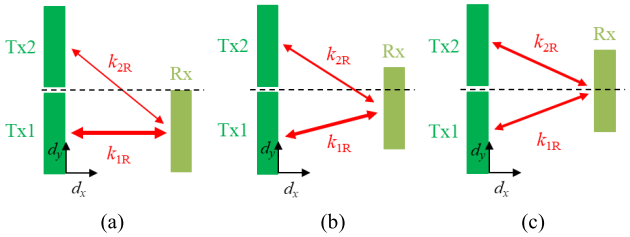

FIGURE 6. Three cases in accordance with Rx position: (a) $d_y = 0$ cm ($k_{1R} > k_{2R}$), (b) $d_y = 2.8$ cm ($k_{1R} > k_{2R}$), and (c) $d_y = 5.75$ cm ($k_{1R} = k_{2R}$).

TABLE 3. Coupling coefficient values at $d_x = 5$ cm.

	k_{1R}	k_{2R}	$\alpha\ (k_{2R}/k_{1R})$	$k_{1R,cri}$
Case#1	0.134	0.004	0.03	0.0239
Case#2	0.108	0.007	0.065	0.0238
Case#3	0.045	0.045	1	0.0169

TABLE 4. Coupling Coefficient Values at $d_x = 8$ cm.

	k_{1R}	k_{2R}	$\alpha\ (k_{2R}/k_{1R})$	$k_{1R,cri}$
Case#1	0.064	0.003	0.047	0.0239
Case#2	0.056	0.011	0.196	0.0234
Case#3	0.028	0.028	1	0.0169

a symmetiric line to satisfy $k_{1R} = k_{2R}$ as shown in Fig. 6 (c). The calculated and measured coupling coeffcient values at $d_x = 5$ cm and 8 cm are shown in Tables III and IV.

We measured the transmission coeffcient S_{21} between Tx1 and Rx in the over-coupled state ($k_{1R} > k_{1R,cri}$), where the conventional system had the resonant capacitances for the operating frequency of 6.78 MHz and the proposed system had the optimum capacitances. The simulated results were obtained by using Keysight's ADS tool. The measured and simulated results are shown in Fig. 7. As predicted, the frequency-splitting phenomenon occurred in all cases. Moreover, the gap between split frequencies increased as the difference between $k_{1R,cri}$ and k_{1R} increased. For all conventional system cases, the transmittion coefficient at 6.78 MHz was reduced by frequency splitting. In particular, in Cases#1 and #2 with the greater frequency shift than Case#3, the transmittion coefficient decreased to −10 dB. On the other hand, the received signal in the proposed system had the

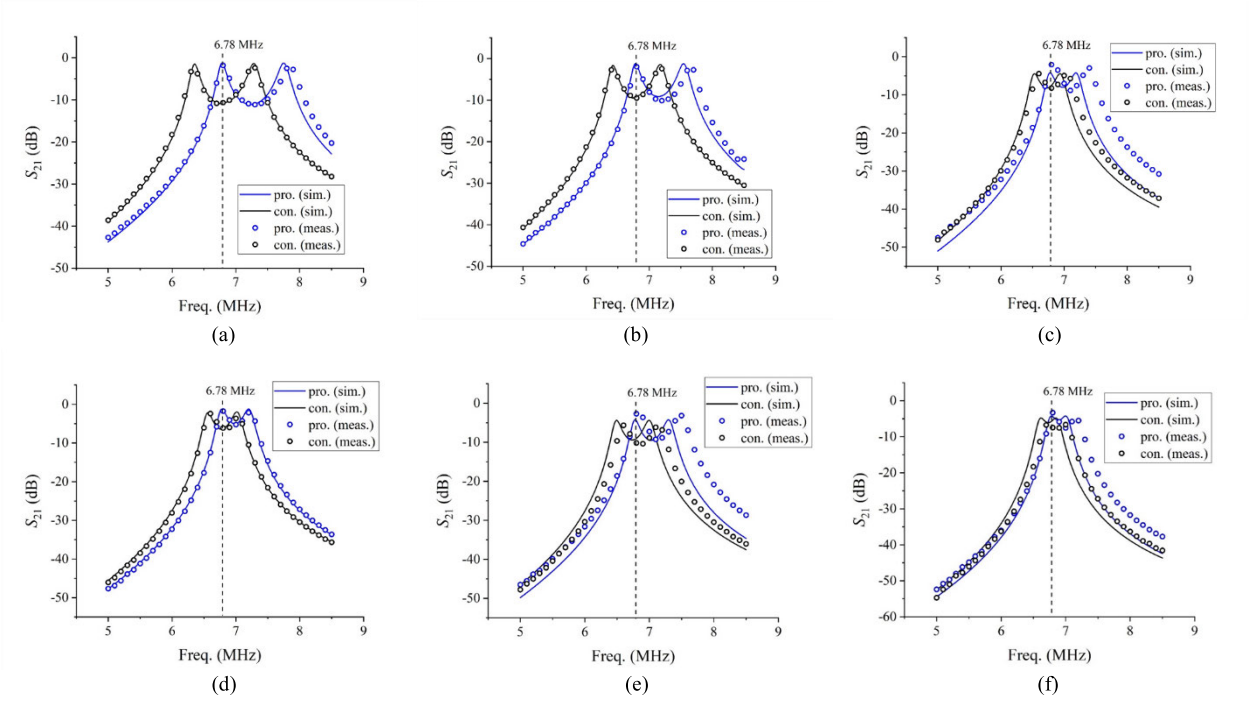

FIGURE 7. Measured and simulated transmission coefficient S_{21} in two-Tx system: when d_x was 5 cm (a) Case#1, (b) Case#2, and (c) Case#3; when d_x was 8 cm (d) Case#1, (e) Case#2, and (f) Case#3.

TABLE 5. Details of experimental setup.

Instrument or Parts	Model or Type	Note
Function generator	WF1948 (2 CH)	up to 30 MHz
Coaxial cable	RG 316	DC-12.4 GHz
Load resistor	Carbon film resistor	2 Ω

peak value at 6.78 MHz in all cases. Although large frequency shifts occurred in Cases#1 and #2, S_{21} was only about −2 dB.

B. EFFICIENCY COMPARISON BETWEEN PHASE AND CAPACITANCE TUNING METHODS

We analyze the transmission efficiency for two- and three-Tx systems tuned with the optimal capacitances according to the Rx position and then compare their performance with that of the conventional phase-controlled system. Figure 8 shows the three-Tx system setup to measure the output power of load. The each power source was implemented with a function generator, and 50-Ω source resistances were matched to the 1-Ω resistance and desired reactance values by using L-section matching networks as shown in Fig. 5. The additional elements and details are summarized in Table V.

To satisfy the optimum current ratio of (2) in the two- and three-Tx systems, the current of each Tx must be adjusted according to the coupling coefficient between the Tx and Rx as shown in Fig. 2. If the coupling coefficient between the i^{th} Tx and Rx is the largest value among the other Txs and Rx, the input power of the n^{th} Tx should be set to $P_{\text{i}} \times (k_{\text{nR}}/k_{\text{iR}})^2$ from the relationship between the current and power, $I^2 \propto P$. For example, the input powers of Tx2 and Tx3 in Fig. 9(a) were set to $P_1 \times (k_{2\text{R}}/k_{1\text{R}})^2$ and $P_1 \times (k_{3\text{R}}/k_{1\text{R}})^2$, respectively,

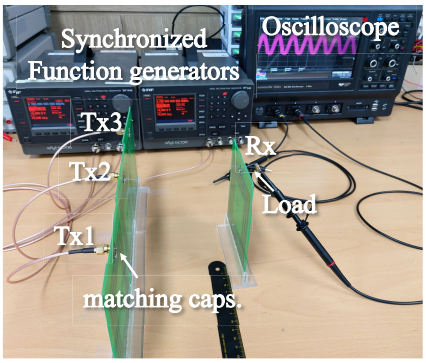

FIGURE 8. Experimental setup for three-Tx system.

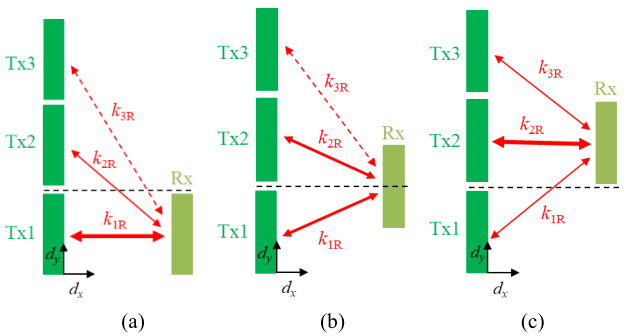

FIGURE 9. Three cases according to the Rx position: (a) $d_y = 0$ cm ($k_{1\text{R}} > k_{2\text{R}} > k_{3\text{R}}$), (b) $d_y = 5.75$ cm ($k_{1\text{R}} = k_{2\text{R}} > k_{3\text{R}}$), and (c) $d_y = 11.4$ cm ($k_{2\text{R}} > k_{1\text{R}} = k_{3\text{R}}$).

because the largest coupling is $k_{1\text{R}}$. We set the largest input power to 10 dBm for the simple power calculation in the experiment and then measured the output power for six cases.

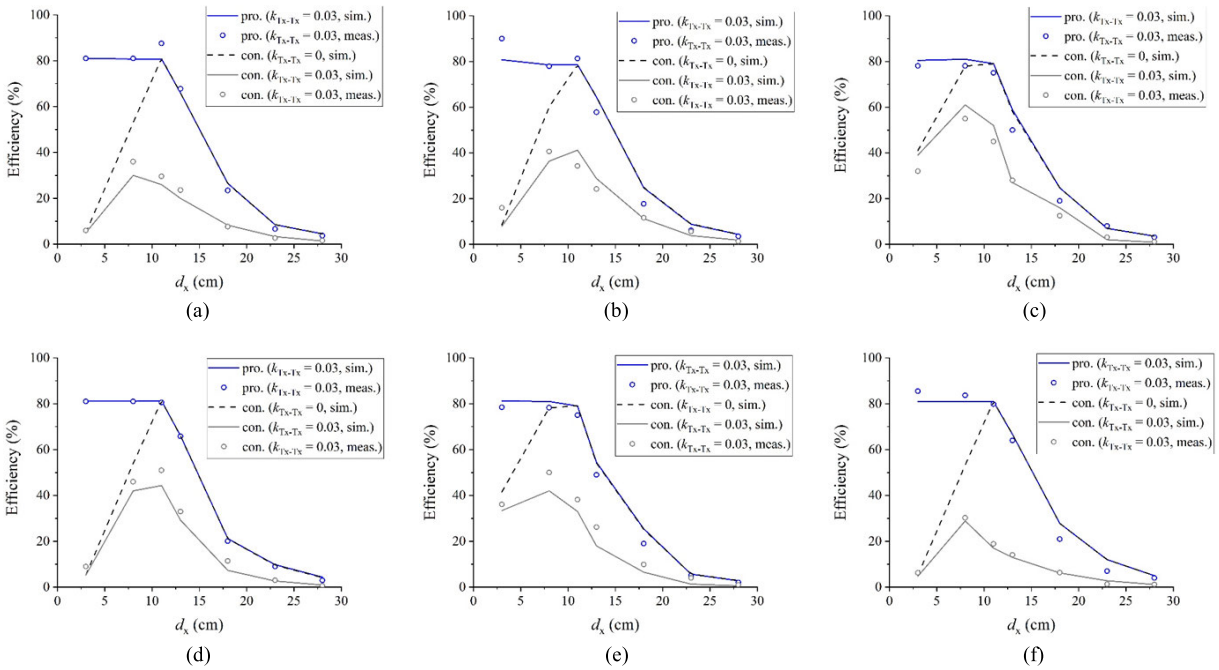

FIGURE 10. Experimental results for transmission efficiency: (a) Case#1, (b) Case#2, and (c) Case#3 in two-Tx system; (d) Case#4, (e) Case#5, and (f) Case#6 in three-Tx system.

Cases#1, #2, and #3 correspond to Fig. 6(a), 6(b), and 6(c) of the two-Tx system, respectively. Cases#4, #5, and #6 correspond to Fig. 9(a), 9(b), and 9(c) of the three-Tx system, respectively.

Figure 10 shows the transmission efficiency of the two- and three-Tx systems with respect to the Rx position along the x- and y-axes. The conventional phase-controlled system was implemented by using [21]. On the other hand, the system without inner coupling between adjacent Txs ($k_{\text{Tx-Tx}} = 0$) was implemented with ADS simulation. For all cases, the transmission efficiency was obtained by the ratio of the output power of load to the total input power, which is the sum of each source.

The results obtained for the two-Tx system showed that the conventional system phase-controlled in each Tx source performed with up to 60% efficiency in Case#3 in which the Rx position is completely centered between Tx1 and Tx2. However, the simulated efficiency of the system with non-inner coupling reaches 80% in the same case. Thus, although the phase control method compensates the signal delay of each Tx, the reactance caused by inner coupling still leads to output power reduction. Moreover, in Cases#1 and #2 with nearly perfect alignment between Tx1 and the Rx, a greater shift of the resonant frequency from the operating frequency occurs in comparison to Case#3 in the over-coupled state, $d_x < 10$ cm. Hence, the conventional system shows poor performance in the over-coupling state as well as the system with non-inner coupling. This means that the conventional multi-Tx system is very vulnerable to the frequency-splitting phenomenon in the over-coupling state. In addition, Cases#4, #5, and #6 in the conventional three-Tx system have lower maximum efficiency than Case#3 in the conventional two-Tx system because the reactance is increased by the additional inner couplings as the number of Txs increases.

On the other hand, the proposed system tuned with optimal capacitances is superior to conventional phase-controlled system in all cases. The efficiency of the proposed system is almost identical to that of the systems with non-inner coupling in the under-coupled state, $d_x > 10$ cm. Moreover, it performs with a constant maximum efficiency, which is about 80% in the over-coupled state, $d_x < 10$ cm. That is, the efficiency of the proposed system is improved such that it is as much as 75% higher than that of the conventional system in the over-coupled state. This means that the multi-Tx system with the proposed optimal capacitances is quite efficient with a wider area than the conventional system.

IV. CONCLUSION

In this article, we proposed an optimal capacitance tuning method for multi-Tx WPT systems. To obtain the optimal capacitances, we derived the critical coupling condition based on transmission efficiency, which achieves the maximum transmission efficiency in a multi-Tx system. With the proposed method, a system tuned with optimal capacitances not only completely compensates the inner coupling among the Txs but also maintains the maximum output power in the over-coupled state. To validate the proposed method, we implemented it with two- and three-Tx systems and then measured the output power of load by changing the Rx position along the x- and y-axes. As a result, the system transmitted higher output power than the conventional phase-controlled system in all cases. In particular, with the

proposed method, the system maintained the constant maximum transmission efficiency of 80% in the over-coupled state.

REFERENCES

[1] J. M. Miller, O. C. Onar, and M. Chinthavali, "Primary-side power flow control of wireless power transfer for electric vehicle charging," *IEEE J. Emerg. Sel. Topics Power Electron.*, vol. 3, no. 1, pp. 147–162, Mar. 2015.
[2] J.-H. Lee and D.-W. Seo, "Development of ECG monitoring system and implantable device with wireless charging," *Micromachines*, vol. 10, no. 1, p. 38, Jan. 2019.
[3] D.-W. Seo, J.-H. Lee, and H. Lee, "Integration of resonant coil for wireless power transfer and implantable antenna for signal transfer," *Int. J. Antennas Propag.*, vol. 2016, pp. 1–7, 2016.
[4] D.-W. Seo, S.-T. Khang, S.-C. Chae, J.-W. Yu, G.-K. Lee, and W.-S. Lee, "Open-loop self-adaptive wireless power transfer system for medical implant," *Micro. Opt. Technol. Lett.*, vol. 58, no. 6, pp. 1271–1275, Jun. 2016.
[5] S. Y. R. Hui and W. W. C. Ho, "A new generation of universal contactless battery charging platform for portable consumer electronic equipment," *IEEE Trans. Power Electron.*, vol. 20, no. 3, pp. 620–627, May 2005.
[6] A. P. Sample, D. A. Meyer, and J. R. Smith, "Analysis, experimental results, and range adaption of magnetically coupled resonators for wireless power transfer," *IEEE Trans. Ind. Electron.*, vol. 58, no. 2, pp. 544–554, Feb. 2011.
[7] M. Soma, D. C. Galbraith, and R. L. White, "Radio-frequency coils in implantable devices: Misalignment analysis and design procedure," *IEEE Trans. Biomed. Eng.*, vol. BME-34, no. 4, pp. 276–282, Apr. 1987.
[8] K. Fotopoulou and B. W. Flynn, "Wireless power transfer in loosely coupled links: Coil misalignment model," *IEEE Trans. Magn.*, vol. 47, no. 2, pp. 416–430, Feb. 2011.
[9] D. Liu, H. Hu, and S. V. Georgakopoulos, "Misalignment sensitivity of strongly coupled wireless power transfer systems," *IEEE Trans. Power Electron.*, vol. 32, no. 7, pp. 5509–5519, Jul. 2017.
[10] S. Ding, W. Niu, and W. Gu, "Lateral misalignment tolerant wireless power transfer with a tumbler mechanism," *IEEE Access*, vol. 7, pp. 125091–125100, Aug. 2019.
[11] F. J. Lopez-Alcolea, J. V. D. Real, P. Roncero-Sanchez, and A. P. Torres, "Modeling of a magnetic coupler based on single- and double-layered rectangular planar coils with in-plane misalignment for wireless power transfer," *IEEE Trans. Power Electron.*, vol. 35, no. 5, pp. 5102–5121, May 2020.
[12] M. Budhia, J. T. Boys, G. A. Covic, and C.-Y. Huang, "Development of a single-sided flux magnetic coupler for electric vehicle IPT charging systems," *IEEE Trans. Ind. Electron.*, vol. 60, no. 1, pp. 318–328, Jan. 2013.
[13] Y. Li, J. Zhao, Q. Yang, L. Liu, J. Ma, and X. Zhang, "A novel coil with high misalignment tolerance for wireless power transfer," *IEEE Trans. Magn.*, vol. 55, no. 6, pp. 1–4, Jun. 2019.
[14] K. Knaisch, M. Springmann, and P. Gratzfeld, "Comparison of coil topologies for inductive power transfer under the influence of ferrite and aluminum," in *Proc. 11th Int. Conf. Ecological Vehicles Renew. Energies (EVER)*, Apr. 2016, pp. 1–9.
[15] T.-H. Kim, G.-H. Yun, W. Y. Lee, and J.-G. Yook, "Asymmetric coil structures for highly efficient wireless power transfer systems," *IEEE Trans. Microw. Theory Techn.*, vol. 66, no. 7, pp. 3443–3451, Jul. 2018.
[16] K. Hatanaka, F. Sato, H. Matsuki, S. Kikuchi, J. Murakami, M. Kawase, and T. Satoh, "Power transmission of a Des. with a cord-free power supply," *IEEE Trans. Magn.*, vol. 38, no. 5, pp. 3329–3331, Sep. 2002.
[17] C. Sritongon, P. Wisestherrakul, N. Hansupho, S. Nutwong, A. Sangswang, S. Naetiladdanon, and E. Mujjalinvimut, "Novel IPT multi-transmitter coils with increase misalignment tolerance and system efficiency," in *Proc. IEEE Int. Symp. Circuits Syst. (ISCAS)*, May 2018, pp. 1–5.
[18] J. Jadidian and D. Katabi, "Magnetic MIMO: How to charge your phone in your pocket," in *Proc. 20th Annu. Int. Conf. Mobile Comput. Netw. (MobiCom)*, 2014, pp. 495–506.
[19] S. Huh and D. Ahn, "Two-transmitter wireless power transfer with optimal activation and current selection of transmitters," *IEEE Trans. Power Electron.*, vol. 33, no. 6, pp. 4957–4967, Jun. 2018.
[20] P. Kong and H. Ku, "Efficiency optimising scheme for wireless power transfer system with two transmitters," *Electron. Lett.*, vol. 52, no. 4, pp. 310–312, Feb. 2016.
[21] B. H. Waters, B. J. Mahoney, V. Ranganathan, and J. R. Smith, "Power delivery and leakage field control using an adaptive phased array wireless power system," *IEEE Trans. Power Electron.*, vol. 30, no. 11, pp. 6298–6309, Nov. 2015.
[22] A. Zaheer, G. A. Covic, and D. Kacprzak, "A bipolar pad in a 10-kHz 300-W distributed IPT system for AGV applications," *IEEE Trans. Ind. Electron.*, vol. 61, no. 7, pp. 3288–3301, Jul. 2014.
[23] Z. Yan, B. Yang, H. Liu, C. Chen, M. Waqas, R. Mai, and Z. He, "Efficiency improvement of wireless power transfer based on multitransmitter system," *IEEE Trans. Power Electron.*, vol. 35, no. 9, pp. 9011–9023, Sep. 2020.
[24] H.-J. Kim, J. Park, K.-S. Oh, J. P. Choi, J. E. Jang, and J.-W. Choi, "Near-field magnetic induction MIMO communication using heterogeneous multipole loop antenna array for higher data rate transmission," *IEEE Trans. Antennas Propag.*, vol. 64, no. 5, pp. 1952–1962, May 2016.
[25] H.-J. Kim, K. Kim, S. Han, D.-W. Seo, and J.-W. Choi, "Nearly non-coupling coil array allowing many independent channels for magnetic communication," *IEEE Access*, vol. 6, pp. 34190–34197, Jun. 2018.
[26] D. Ahn and S. Hong, "Effect of coupling between multiple transmitters or multiple receivers on wireless power transfer," *IEEE Trans. Ind. Electron.*, vol. 60, no. 7, pp. 2602–2613, Jul. 2013.
[27] M. Fu, T. Zhang, X. Zhu, P. Chi-Kwong Luk, and C. Ma, "Compensation of cross coupling in multiple-receiver wireless power transfer systems," *IEEE Trans. Ind. Informat.*, vol. 12, no. 2, pp. 474–482, Apr. 2016.
[28] S. B. Lee, M. Kim, and I. G. Jang, "Determination of the optimal resonant condition for multi-receiver wireless power transfer systems considering the transfer efficiency and different rated powers with altered coupling effects," *IEEE J. Emerg. Sel. Topics Power Electron.*, early access, Mar. 27, 2020, doi: 10.1109/JESTPE.2020.2983824.
[29] S. Kong, M. Kim, K. Koo, S. Ahn, B. Bae, and J. Kim, "Analytical expressions for maximum transferred power in wireless power transfer systems," in *Proc. IEEE Int. Symp. Electromagn. Compat.*, Aug. 2011, pp. 379–383.
[30] R. Huang, B. Zhang, D. Qiu, and Y. Zhang, "Frequency splitting phenomena of magnetic resonant coupling wireless power transfer," *IEEE Trans. Magn.*, vol. 50, no. 11, pp. 1–4, Nov. 2014.
[31] D.-W. Seo, "Comparative analysis of two- and three-coil WPT systems based on transmission efficiency," *IEEE Access*, vol. 7, pp. 151962–151970, Oct. 2019.
[32] J. Zhang, C. Cheng, K. Chen, F. Wang, and Y. Gao, "Analysis of multiple-TX WPT systems using KVL and RX-side RLT," *IET Microw., Antennas Propag.*, vol. 13, no. 12, pp. 1997–2004, Oct. 2019.
[33] D.-H. Kim and D. Ahn, "Maximum efficiency point tracking for multiple-transmitter wireless power transfer," *IEEE Trans. Power Electron.*, vol. 35, no. 11, pp. 11391–11400, Nov. 2020.
[34] Z. Bi, T. Kan, C. C. Mi, Y. Zhang, Z. Zhao, and G. A. Keoleian, "A review of wireless power transfer for electric vehicles: Prospects to enhance sustainable mobility," *Appl. Energy*, vol. 179, pp. 413–425, Oct. 2016.
[35] K. Aditya and S. S. Williamson, "A review of optimal conditions for achieving maximum power output and maximum efficiency for a series–series resonant inductive link," *IEEE Trans. Transport. Electrific.*, vol. 3, no. 2, pp. 303–311, Jun. 2017.
[36] H. L. Li, A. P. Hu, G. A. Covic, and C. S. Tang, "Optimal coupling condition of IPT system for achieving maximum power transfer," *Electron. Lett.*, vol. 45, no. 1, pp. 76–77, Jan. 2009.
[37] D.-W. Seo, J.-H. Lee, and H.-S. Lee, "Optimal coupling to achieve maximum output power in a WPT system," *IEEE Trans. Power Electron.*, vol. 31, no. 6, pp. 3994–3998, Jun. 2016.
[38] M. Wagih, A. Komolafe, and B. Zaghari, "Dual-receiver wearable 6.78 MHz resonant inductive wireless power transfer glove using embroidered textile coils," *IEEE Access*, vol. 8, pp. 24630–24642, Feb. 2020.
[39] K.-S. Yoon, S.-H. Lee, I.-K. Cho, H.-J. Lee, and G.-H. Cho, "Dual receiver coils wireless power transfer system with interleaving switching," *IEEE Trans. Power Electron.*, vol. 33, no. 12, pp. 10016–10020, Dec. 2018.
[40] D. M. Pozar, *Microwave Engineering*, 4th ed. Hoboken, NJ, USA: Wiley, 2011, ch. 4.3.